Desalination and Water Treatment
www.deswater.com
doi: 10.5004/dwt.2021.27795

243 (2021) 211–220
December

Permanent magnet treatment technology for crystal blockage of tunnel drainage pipes

Hao Leng[a], Huoyin Lv[b], Fenglei Han[c,d,*], Fabo Liu[a], Tao Liu[c,d]

[a]*Sichuan Lehan Expressway Co., Ltd., Leshan 614200, China*
[b]*CCTEG Chongqing Engineering (Group) Co., Ltd., Chongqing 400039, China*
[c]*State Key Laboratory of Mountain Bridge and Tunnel Engineering, Chongqing 400074, China, email: hanfl2017@cqjtu.edu.cn (F. Han)*
[d]*College of Civil Engineering, Chongqing Jiaotong University, Chongqing 400074, China*

Received 17 August 2021; Accepted 23 September 2021

ABSTRACT

The tunnel drainage pipes located in karst areas are oftentimes subject to crystallization and clogging derived from the calcification in groundwater, which would result in poor tunnel drainage during operation as well as subsequent issues such as cracking of the lining structure and seepage/leakage caused by rising levels of groundwater. To address the issue of crystallization in tunnel drainage pipes located in karst areas, we have examined the patterns of $CaCO_3$ crystallization taken place in tunnel drainage pipes based on the intensity of the magnetic field, rate of water flow, and pipe materials. We have adopted the control variable method according to laboratory model experiments, X-ray diffraction, and scanning electron microscopy, and we have drawn reference from the principle of magnetic descaling applied in industry. Our research findings indicate that the mass of crystals in the drainage pipes would experience gradual increases and tend to stabilize with the test cycle, whereas the total mass of such crystals would decrease first before increasing with the intensity of the magnetic field. In addition, the mass of crystals was measured to be the smallest when the intensity of the magnetic field amounted to 0.2 T, whereas the rate of scale inhibition amounted to 30.78% of the crystal mass in the pipes without the magnetic field. Results of the micro-morphological analysis indicate that under the magnetic field, the $CaCO_3$ crystals have been through the transition of its form from stable calcite to loose and unstable aragonite given that they are subject to the molecular orientation effect. The mass of crystals in the experimental pipes was found to increase in accordance with the test cycle and the increase of the water flow rate. In addition, under the intensity of the magnetic field amounting to 0.2 T, the final maximum mass of crystals in the pipe experienced a decline of 30.54% compared with that in the pipe under normal conditions. Judging from the experimental results, the materials applied in the steel-plastic composite pipe could, better address the issue of the weak magnetic field in some areas of the pipe to some extent, but they were unable to play a critical role in inhibiting crystallization. In general, the crystallization was found to be inhibited in those drainage pipes under the magnetic field, and the mass of crystals was to decrease correspondingly. Through this study, we aim to lay a foundation for the design, construction and remediation for applying the magnetic fields into the inhibition of crystallization in tunnel drainage pipes located in karst regions.

Keywords: Karst tunnel; Crystallization in drainage pipes; Magnetic descaling; Water flow rate; Pipe material

* Corresponding author.

1. Introduction

As the infrastructure related to highway transportation experienced robust growth in China, tunnels have increasingly been built in karst areas, accounting for an evidently larger proportion. The groundwater in karst areas is rich in Ca^{2+} and HCO_3^-, and is capable of generating $CaCO_3$ precipitates under certain hydrodynamic conditions (the specific formula of reaction is specified as Eq. (1)), leading to the crystallization and clogging of $CaCO_3$ in drainage pipes during the operation of tunnel building in karst areas [1,2]. In addition, such crystallization and clogging take place in tunnel drainage pipes in karst areas could result in higher water pressure, leading to seepage/leakage and lining cracking in tunnels. Along with the corrosion caused by karst groundwater, they might lead to catastrophic consequences derived from secondary lining penetration [3,4].

$$Ca^{2+} + 2HCO_3^- \rightarrow CaCO_3 \downarrow + CO_2 \uparrow + H_2O \quad (1)$$

Numerous studies have been carried out on the issue of crystallization and clogging of $CaCO_3$ in tunnel drainage pipes. Liu et al. attached flocking to the inner wall of drainage pipes for polyvinylidene chloride (PVC), and through the drainage experiments, they found that due to the peristaltic movement of villi, $CaCO_3$ crystals became less likely to adhere, thereby effectively preventing the crystallization and clogging from occurring in PVC drainage pipes [5–8]. A studied the effect imposed by numerous water-filling states on crystallization under varying alkaline conditions [9]. Applied a unique material into drainage pipes so as to minimize the crystal precipitation [10]. Examined the effects imposed by several tube materials, such as PVC and polytetrafluoroethylene (PTFE), on the accumulation and precipitation of crystals [11]. Based on their study and analysis of mechanisms as well as experiments, found that crystallization and clogging taken place in tunnel drainage pipes is closely linked with shotcrete [12–15]. To reduce the amount of dissolved calcium by 65% compared to that of normal mix concrete by optimizing the mix proportion of shotcrete [16]. Conducted the statistical analysis on a large number of tunnels located in France that are plagued with the issue of calcite precipitation, and found that the issue was linked with the lining materials and geometry of tunnels [17]. Studies on $CaCO_3$ crystals, which are commonly known as scale in daily life, began relatively late in the field of tunnel building. Nevertheless, numerous studies have been carried out on addressing the issue of scale in industrial water, thus providing a reference for the treatment of crystallization and clogging taken place in tunnels [18–20]. Commonly used methods of scale prevention and control include physical and chemical approaches, biological approaches, and integrated approaches. Commonly used physical methods of descaling include the magnetic, electric and ultrasonic treatment approaches [21]. In general, the magnetic treatment can be divided into two categories, namely, the permanent magnet treatment and the high-frequency electromagnetic treatment [22]. Carried out the research on scale inhibition and removal by adopting permanent magnets in the textile field [23]. In addition, the rate of crystallization scaled up, but the amount of adhesion on pipe walls decreased by 25.6% [24–28]. The relationship between the magnetic induction intensity and the amount of scale through experiments, and put forward the concept of the "threshold of magnetic induction for scaling" [29]. Through the experimental study, found that the magnetic treatment would contribute to the reduction of the scaling rate of the circulating cooling water in power plants by 96% [30]. The research results indicate that the magnetic field could alter the reaction process between the ions that form crystals in solution as well as the type of crystals formed, whereas the magnetic field could lead to the transition of the crystal form of $CaCO_3$ from calcite to aragonite [31–34].

To sum up, we have found that magnetic fields could be used to treat scale in such areas as industrial water circulation. However, few studies have been conducted on the use of magnetic fields for preventing crystallization from taking place in tunnel drainage pipes. In this study, we have adopted the control variable method to examine the patterns of crystallization in tunnel drainage pipes based on the intensity of the magnetic field, the rate of water flow and the drainage pipe material through laboratory model experiments. In addition, we have analyzed the optimal intensity of magnetic field for scale inhibition so as to lay a foundation for the design, construction and application of permanent magnets in preventing crystallization from taking place in the tunnel drainage pipes in karst areas.

2. Experiment

2.1. Objective and concept

To gain insights into the patterns of crystallization taken place in tunnel drainage pipes under the action of permanent magnets, we have carried out the design on laboratory simulation experiments to study the effects imposed by three factors (namely, the intensity of the magnetic field, rate of flow and pipe material) on the crystallization of $CaCO_3$ in tunnel drainage pipes, and we have analyzed the effects imposed by the magnetic field of the permanent magnet on preventing and eliminating crystals under varying influencing factors. Subsequently, we have identified the optimal parameters of the magnetic field according to its impact on crystallization and clogging in tunnel drainage pipes. We have first conducted experiments on the intensity of the magnetic field to obtain the optimal magnetic field before examining the flow rate and pipe material under the optimal magnetic field.

2.2. Materials and apparatus

Materials adopted in the experiment mainly include high-strength tegular permanent magnets (with a length of 10 cm), analytical calcium chloride ($CaCl_2$), analytical pure sodium bicarbonate ($NaHCO_3$), a water pump (with a head of 3 m), a water tank, smooth PVC pipes with a diameter of 50 mm, steel-plastic composite pipes, matching straight connectors, elbow connectors and ball valves. The apparatus utilized in the experiment mainly include an ultrapure water machine, a drying oven, measuring cylinders, Gauss meters, and a high-precision electronic balance.

2.3. Design parameters

The parameters adopted in the experiment mainly include the intensity of the magnetic field, spacing of permanent magnet, rate of water flow, and material of drainage pipes.

2.3.1. Intensity of magnetic field and spacing of permanent magnets

The magnetic field inside the experimental pipes was generated by high-strength tegular permanent magnets with an inner diameter of 50 mm. The intensity of the magnetic field was found to increase at a gradually declining rate as the number of magnets increased, whereas the magnetic field was approximately linear with the number of magnets ranging between 0.1 and 0.4 T (Table 1). Therefore, the intensity of the magnetic field selected for the laboratory model experiments amounted to 0.0, 0.1, 0.2, 0.3 and 0.4 T, respectively.

The experimental findings indicate that a smaller spacing between the permanent magnets would result in a more uniform distribution of the magnetic field. However, the magnet spacing is not advised to be overly narrow given that the interactive force would exist between the magnets. Judging from our measurements and experiments several times, the magnetic field was rather stable when the spacing between the permanent magnets ranged between 8 and 10 cm. Therefore, we have eventually opted for the magnet spacing of 10 cm. The layout of the experimental pipes is illustrated in Fig. 1.

2.3.2. Water flow rate

In this study, we have adopted the pump with a head of 2.5 m. We have controlled the flow rate in the pipe mainly through the valve at the outlet of the pump. During the preliminary pre-test study, we have found that the maximum flow rate amounted to approximately 700 mL/s under circumstances of the full pipe flow. Therefore, we have opted for parameters of the flow rate with a distribution ranging between 0 and 700 mL/s in the experiment. Subsequent to our holistic review, we have opted for the rate of 150 mL/s as the increment to obtain four levels of parameter values for the flow rate, namely, 150, 300, 450, and 600 mL/s.

2.3.3. Drainage pipe material

Since iron features a high magnetic permeability and is easily magnetized to review certain magnetic properties, we have selected pipe materials commonly used as tunnel drainage pipes in this study, namely, PVC pipes and steel-plastic composite pipes with iron cores, which are commonly available in the market.

2.4. Experimental setup

The experimental setup is illustrated in Fig. 2. The solution used in the experiment was a freshly prepared solution of saturated calcium bicarbonate ($Ca(HCO_3)_2$). While passing through the pump, the solution was dependent on the ball valve for the control of the flow rate. Subsequently, the solution flowed through the experimental section and eventually returned to the tank. Varying levels of intensity of magnetic field could impose different effects on the solution, and thus we have conducted each set of experiments on the intensity of magnetic field separately in a tank, so as to avoid mutual interference. In addition, the intensity of magnetic field that we have selected for the experiments on the flow rate and pipe material have shown consistency; therefore, we have placed the four sets of experimental pipes in the same experimental setup.

Table 1
Relationship between the number of magnets and the magnetic field intensity

Number of permanent magnets	Magnetic field strength (mT)	Number of permanent magnets	Magnetic field strength (mT)
1	112.8	4	384.6
2	206.8	5	440.6
3	295.5	6	455.8

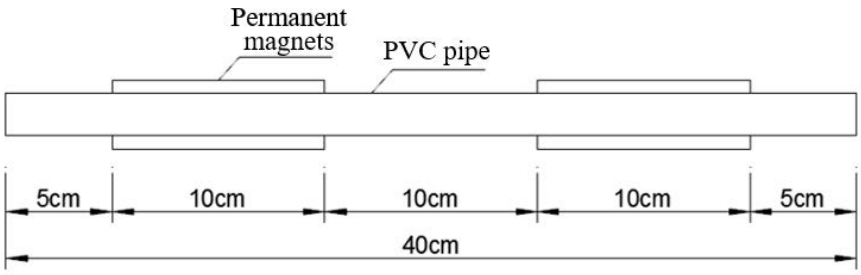

Fig. 1. Schematic diagram of the test pipe section.

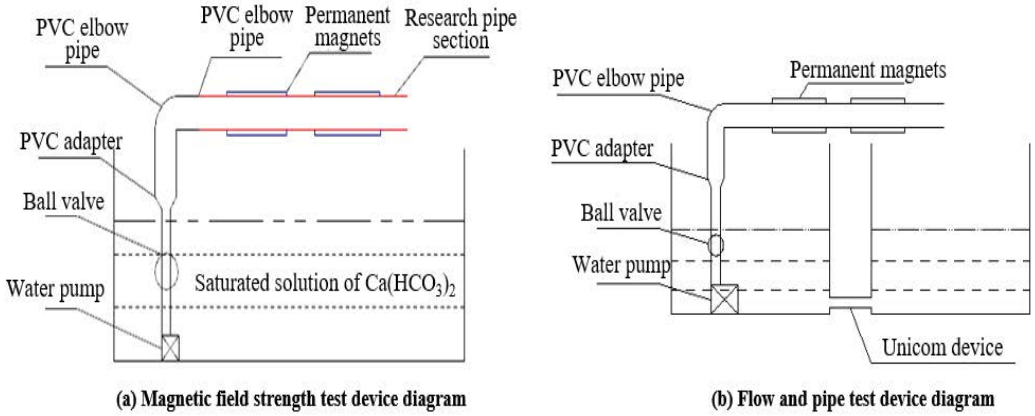

Fig. 2. Schematic diagram of the test device.

In addition, we have adopted four sets of control groups with the same flow rate and without a magnetic field.

2.5. Experimental period

The experimental period lasted for 56 d and was divided into eight cycles, each lasting for 7 d, for measurements of the crystal mass. Subsequent to each cycle, we have removed the experimental pipe from the setup and dried the pipe to a constant mass. In addition, we have ensured that the air was cooled to room temperature and weighed the pipe by using the electronic balance and record, and we have reconnected the pipe to the experimental setup for the next experimental cycle.

3. Results and discussion

The mass of crystals refers to the difference between the mass of the drainage pipe subsequent to the drying in a cycle and the original mass. To assess the inhibition effect imposed by the intensity of magnetic field on crystallization in the drainage pipes, we have calculated the rate of crystallization inhibition for each experimental cycle based on Eq. (2).

$$\phi = \frac{m_1 - m_2}{m_1} \times 100\% \quad (2)$$

where m_1 and m_2 refer to the masses of the crystals from the control group (without application of the magnetic field) and the experimental group (with application of the magnetic field), respectively, at a certain moment in time.

3.1. Intensity of magnetic field

We have utilized a normal PVC pipe during the experiment with a flow rate of 450 mL/s and an experimental period lasting for 56 d. Judging from Fig. 3, the crystal mass of the control group (i.e., the group without the magnetic field) was smaller than that of the experimental group (i.e., that with the magnetic field) on Day 7, contributing to the maximum difference of 0.40 g in the crystal mass. In addition, the ϕ value of each experimental group was less than 0, indicating that the magnetic field could impose a promotion effect on crystallization during the early stage of the experiment. This result was mainly derived from the fact that anions and cations in the solution moved in opposite directions under the magnetic field. Correspondingly, they would collide with each other on a more frequent basis, contributing to the formation of a large quantity of $CaCO_3$ crystals within a short period of time after the anions and cations entered into the magnetic field. When the intensity of magnetic field amounted to 0, the mass of crystals in the drainage pipes would basically experience linear increases with time. When the intensity of magnetic field exceeded 0, the growth rate of the crystals in the drainage pipes would experience gradual declines with time. The contributing factor behind is that under a magnetic field, $CaCO_3$ is prone to form loosely structured aragonite instead of densely structured calcite, and it would become harder for it to adhere to the drainage walls so as to form crystals. In particular, after Day 42, the growth rate of crystals in the experimental group at the intensity of magnetic field of 0.4 T experienced abrupt increases, possibly because the growth of crystals contributed to the increased friction of the inner wall of the drainage pipe, facilitating the adherence of crystals to the wall. By comparing this group with other experimental groups, we have found that the crystal masses in each of the cycles and at the end of the experiment were measured to be minimal when the intensity of magnetic field amounted to 0.2 T, and were measured to be maximal when the intensity of magnetic field amounted to 0.4 T. The crystallization inhibition was found to achieve an optimal effect when the intensity of magnetic field amounted to 0.2 T, whereas the corresponding crystal mass amounted to 1.53 g lower than the final crystal mass in the pipe without the magnetic field, leading to a rate of crystallization inhibition of 30.78%. At an intensity of magnetic field of 0.4 T, the crystal growth was substantially enhanced, whereas the crystal mass increased by 9.46% compared with that in the pipe without the magnetic field. Our research findings indicate that the magnetic field would impose an inhibiting effect on $CaCO_3$ crystallization when

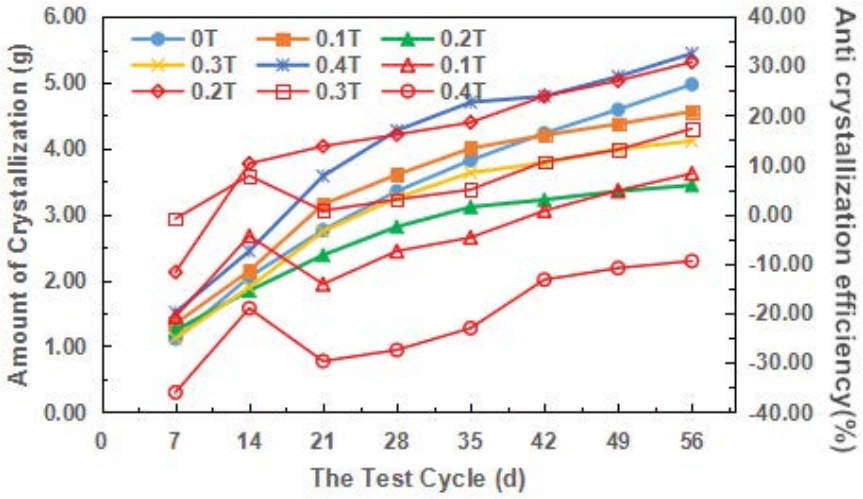

Fig. 3. Relationship between crystallization amount and anti-crystallization efficiency of drainage pipe and test time.

the intensity of magnetic field fell within a certain range, while imposing a promotion effect on $CaCO_3$ crystallization when the intensity of magnetic field was excessively high.

We have carried out the X-ray diffraction (XRD) analysis to evaluate the composition of the crystals in the drainage pipes under varying levels of intensity of magnetic field. Judging from Fig. 4, the crystals in the drainage pipes under varying levels of intensity of magnetic field have shown basically the same diffraction patterns. The XRD spectra of the crystals in each experimental

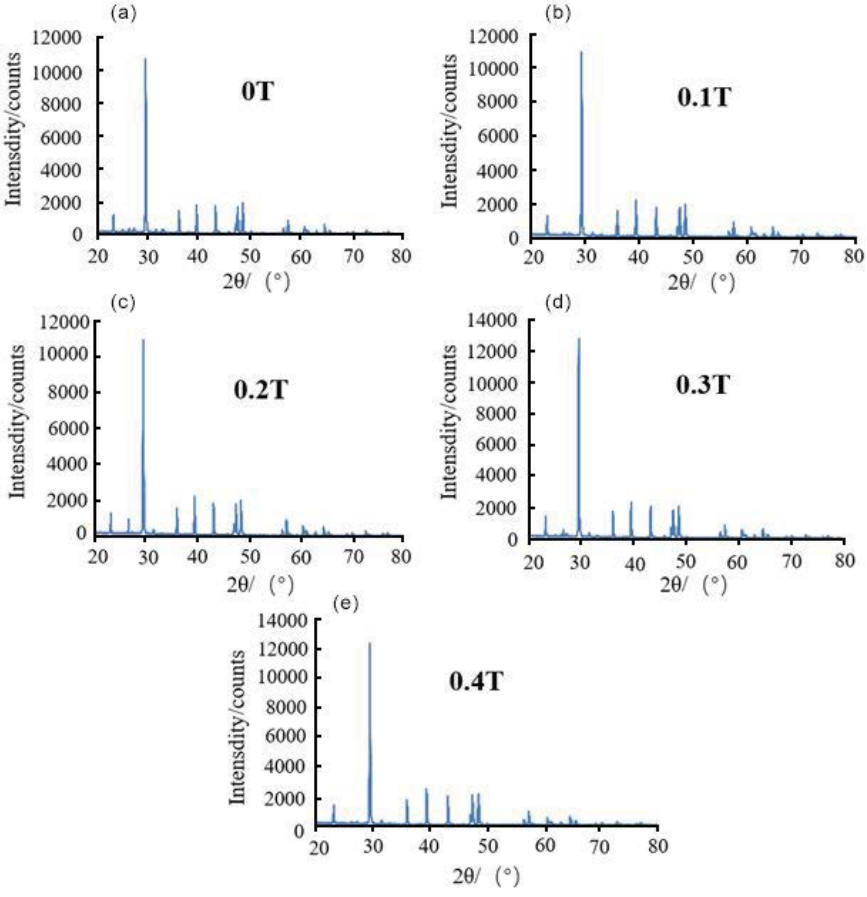

Fig. 4. XRD analysis pattern of crystals (a) 0 T, (b) 0.1 T, (c) 0.2 T, (d) 0.3 T, and (e) 0.4 T.

pipe have shown a peak, with a maximum intensity at 2θ of 29°, whereas the corresponding 2θ values for calcite, aragonite, and vaterite $CaCO_3$ crystals amounted to 29°, 26°, and 46°, respectively, indicating that the crystals were mainly composed of calcite. No evident peak has been formed at 2θ of 26° or 46°, indicating that there was an extremely low content of aragonite and vaterite in the crystals, which was basically in consistence with the composition of the crystalline materials measured in the field. Since the magnetic field could not alter the crystal form or morphology of the $CaCO_3$ product, the magnetic field have imposed an impact on crystallization mainly by inhibiting the formation of $CaCO_3$. In addition, given that the aragonite under the magnetic field was formed in a loose and unstable state, it could be easily washed away under the water flow, whereas the remaining crystals were calcite.

We have analyzed the microscopic morphology of the crystals formed under varying levels of intensity of magnetic field through the scanning electron microscopy (SEM) approach to examine the effects imposed by the magnetic field on the crystal form of $CaCO_3$.

In Fig. 5, we have illustrated the SEM images of the crystals for each experimental group at a magnification of 2,000X. The crystals in the pipes without the magnetic field

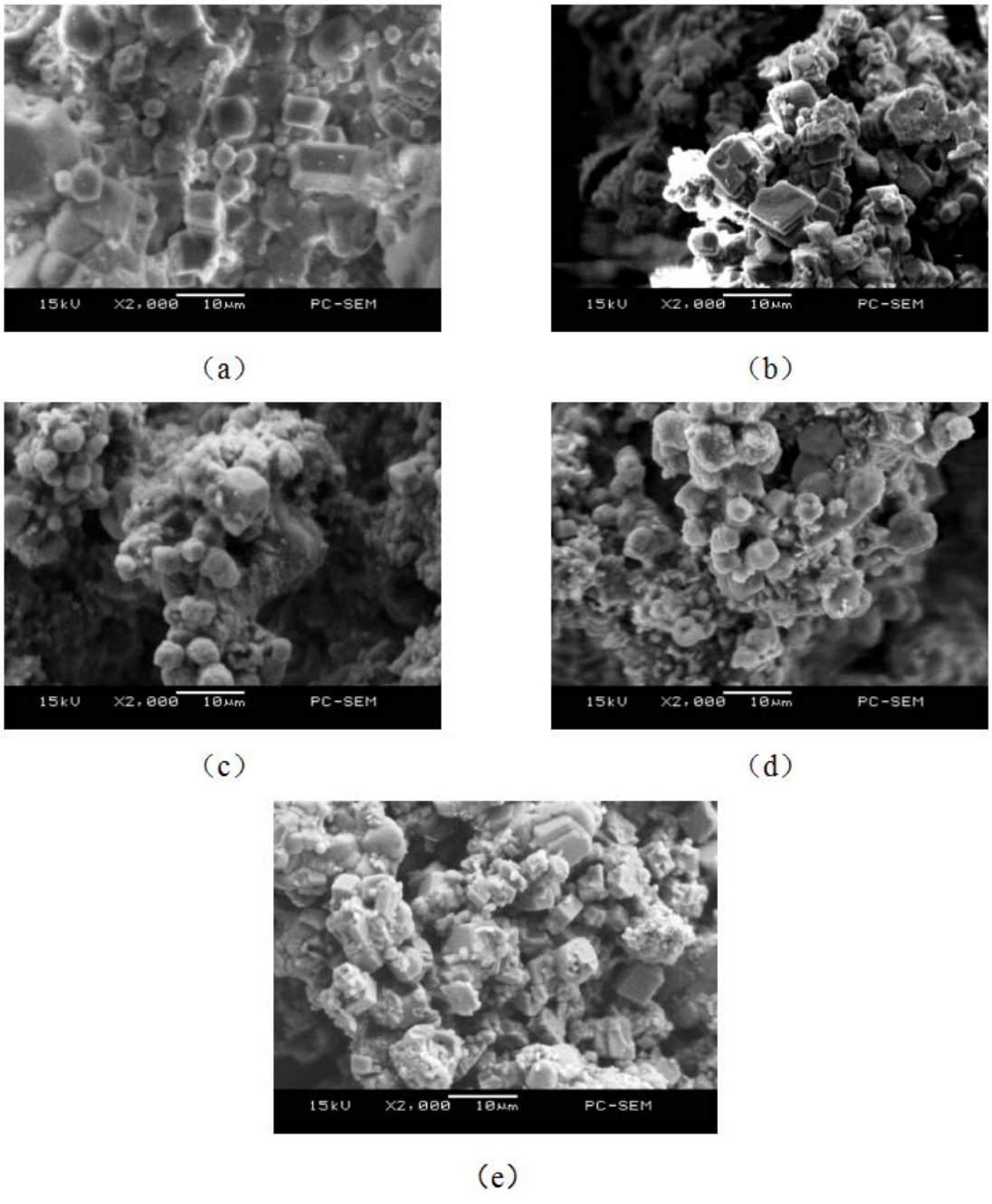

Fig. 5. SEM scanning results of crystals (a) 0 T, (b) 0.1 T, (c) 0.2 T, (d) 0.3 T, and (e) 0.4 T.

mostly featured a regular cubic shape with varying sizes of grain, and were tightly packed with no evident gaps. When the intensity of magnetic field amounted to 0.1 T, some of the crystals in the experimental pipes commenced to show irregular shapes with rough edges and corners. In addition, gaps were found to exist between crystals, leading to the reduced compactness. When the intensity amounted to 0.2 T, the crystals basically featured an irregular spherical shape, and overall, the crystals featured small sizes of grain and were loosely arranged. When the intensity amounted to 0.3 T, the crystals featured irregular spherical and cubic shapes, and they were interlaced and loosely arranged; in the meantime, numerous grains of small sizes were attached to the surface of crystals. When the intensity amounted to 0.4 T, a portion of the crystals were restored to a regular cubic shape, with crystal grains of small sizes attached to the surface. Judging from the SEM images, the standard calcite featured a regular cubic shape, whereas the aragonite and vaterite featured an irregular spherical or striped shape, revealing the tendency of calcite crystals to being transformed into aragonite or spherulite under the magnetic field. Under such circumstance, the intensity of magnetic field could alter the shape, size of grains and the compactness of the $CaCO_3$ crystals.

3.2. Water flow rate

Based on the experiments of crystallization in the drainage pipes under varying levels of intensity of magnetic field, we have carried out experiments of crystallization in the pipes under different rates of water flow at a magnetic field intensity of 0.2 T. Fig. 6 shows the variation pattern of the crystal growth in the pipes under varying flow rates. In each experimental cycle, the mass of crystals in the pipes would increase correspondingly as the flow rate increased. After 65 d at a magnetic field intensity of 0.0 and 0.2 T, the experimental group under a flow rate of 600 mL/s featured a crystal mass of 5.49 and 3.93 g, respectively, in the drainage pipe, which amounted to 25.16% and 53.35% more than that under a flow rate of 150 mL/s. Judging from Fig. 6, at a magnetic field intensity of 0.2 T in the experimental cycle of 7 d, the rate of crystallization inhibition would increase as the rate of water flow rate decreased. For instance, the optimal effect of inhibition under a flow rate of 150 mL/s amounted to 18.18%, while merely a minor promotion effect was imposed on crystallization in drainage pipes under a flow rate of 450 mL/s. This research result was derived from the promotion effect imposed by the magnetic field on the formation of $CaCO_3$ in the short term, whereas under the flow rate of 450 mL/s, a large quantity of crystals were already generated before the flow rate grew larger, accounting for the insufficient hydrodynamic force. On Day 56, under the magnetic field in the drainage pipe, the rate of crystallization inhibition would first increase before declining as the flow rate increased. Compared to the mass of crystals in the pipe without a magnetic field, the final mass of crystals in the pipe that were subject to a magnetic field under flow rates of 150, 450, and 600 mL/s decreased by 12.29%, 30.54% (which is deemed to achieve the optimal effect of crystallization inhibition), and 28.41%, respectively, indicating the potential presence of a certain threshold of flow rate. When the threshold is surpassed, the effect imposed by the magnetic field on crystallization inhibition would diminish instead of growing with the increase of the flow rate. The reason behind is that when the flow rate was low, the magnetic field played a dominant role in inhibiting crystallization by altering the morphology of $CaCO_3$, and thus the loosely arranged crystals in the magnetic field could be discharged. Under such circumstances, the tightly arranged crystals in the pipes without a magnetic field would be merely subject to a minor impact. On the other hand, when the flow rate was sufficiently large, the crystals in the pipes without a magnetic field could be discharged with the water flow, and thus the flow rate would play a dominant role in this case.

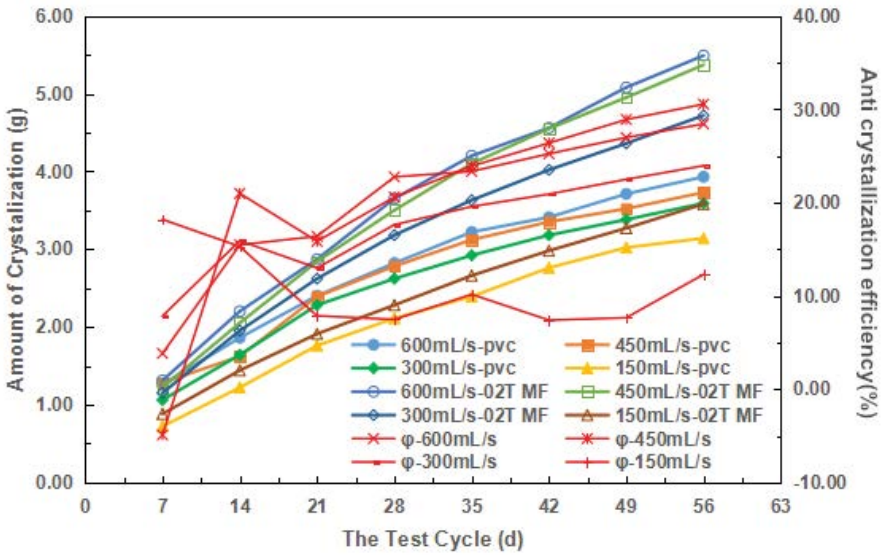

Fig. 6. Variation of crystallization amount and anti-crystallization efficiency of drainage pipe with test time under different flow rates.

3.3. Drainage pipe material

According to the numerical simulation, we have examined the effects imposed by the intensity and spacing of the permanent magnets on the distribution of magnetic field, as illustrated in Fig. 7. Inevitably, parts of the pipe were found to feature a relatively low level of magnetic field intensity (e.g., zones B and C) between two sets of permanent magnets, thereby contributing to the non-uniform distribution of magnetic field intensity in the pipe. However, it is infeasible to enhance the intensity of magnetic field of these two parts to a significant extent by increasing the magnetic field intensity of the permanent magnets or by narrowing their spacing. Given that iron can be easily magnetized to feature certain magnetic properties, we have adopted steel-plastic composite pipes with iron interlayers and ordinary PVC pipes during the experiment. In addition, we have opted for the magnetic field intensity of 0.2 T and the flow rate of 450 mL/s.

The experimental results are illustrated in Fig. 8. Overall, the final mass of crystals in the steel-plastic composite pipe was merely slightly larger (by 3.42%) than that in the ordinary PVC pipe, whereas the mass of crystals did not decrease subsequent to the magnetization of the interlayer in the steel-plastic composite pipe. The research result is potentially because such magnetization by the permanent magnets failed to reach a level that could affect $CaCO_3$ crystallization. Therefore, the inhibition effects of the two types of pipe materials on $CaCO_3$ crystallization did not differ with each other to a significant extent.

4. Conclusions

We have carried out laboratory experiments to study the patterns of crystallization in tunnel drainage pipes at varying levels of magnetic field intensity (0, 0.1, 0.2, 0.3, and 0.4 T), under varying flow rates (150, 300, 450, and 600 mL/s), and with the use of different sorts of pipe materials (PVC and steel-plastic composite). Through our research, we have drawn the following conclusions:

- In a certain range of intensity of magnetic field, the magnetic field could play an inhibition role on the $CaCO_3$ crystallization, whereas an excessively large intensity of magnetic field could impose a promotion effect on the $CaCO_3$ crystallization. The crystallization inhibition was able to achieve an optimal effect at a magnetic field intensity of 0.2 T, whereas the corresponding final mass of crystals amounted to 1.53 g less than that in the pipe without a magnetic field, indicating a rate of crystallization inhibition rate reaching 30.78%.
- Calcite crystals tended to be transformed into aragonite or vaterite under a magnetic field, and the intensity of magnetic field could alter the shape, size of grains and compactness of $CaCO_3$ crystals.

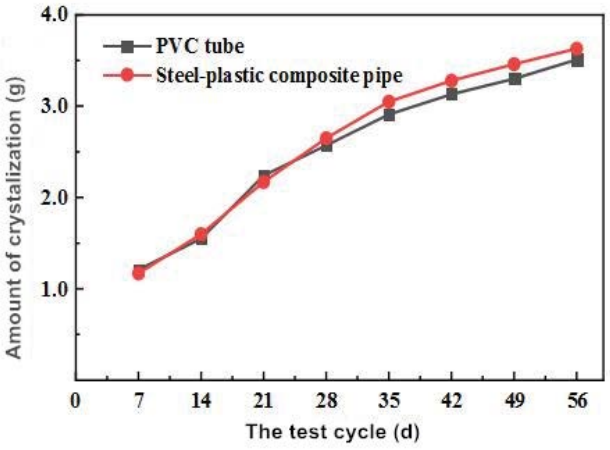

Fig. 8. Growth trend of crystallinity in different pipe tests.

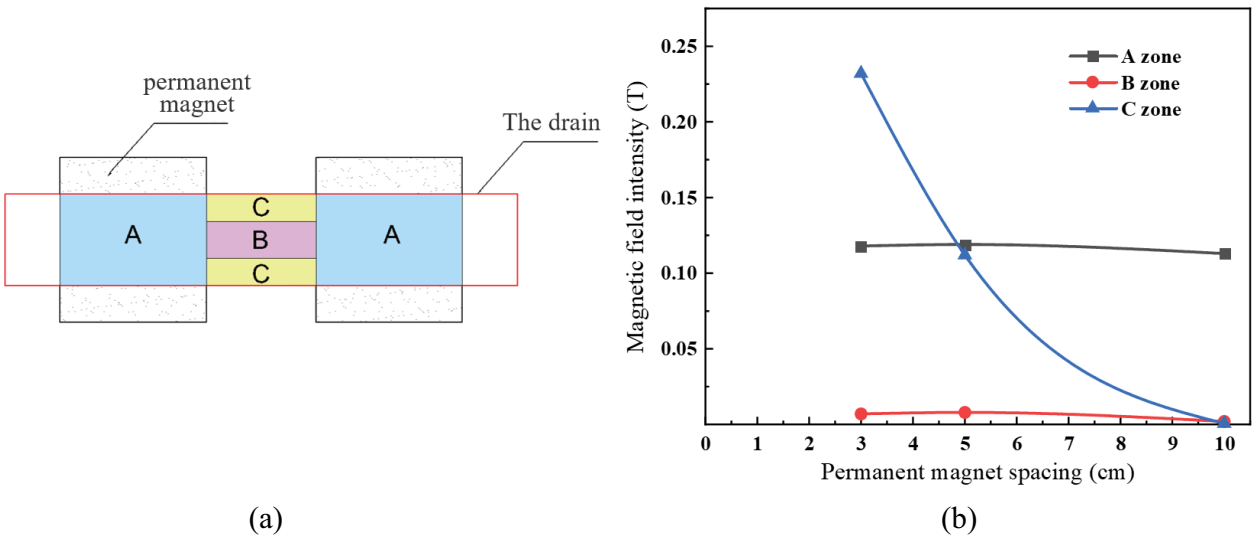

Fig. 7. Magnet spacing and magnetic field intensity: (a) Magnetic field division and (b) Variation of magnetic field intensity in different regions with the distance between permanent magnets.

- In a certain range of flow rates, the descaling rate tended to increase as the flow rate grew larger. In addition, when the flow rate reached a certain threshold, the rate of crystallization inhibition would cease to increase as the flow rate increased.
- During the experiment on varying pipe materials, magnetization of the interlayer of the steel-plastic composite pipe failed to facilitate the reduction of the mass of crystals. Therefore, the inhibition effects imposed by the two pipe materials (PVC and steel-plastic composite) on $CaCO_3$ crystals were not discrepant to a significant extent.

Ethical compliance

There is no research experiment conducted in this article with animals or humans.

Conflicts of interest

The authors declare no conflicts of interest.

Acknowledgements

This research was financially supported by the Scientific Research Project of the Emei Hanyuan Expressway Project (Grant No. LH-HT-45), and the Science and technology project of Guizhou Provincial Department of transportation (Grant No. 2017-123-011).

References

[1] M.E. Botello-Zubiate, A. Alvarez, F. Almeraya Calderon, J.A. Matutes-Aquino, Influence of magnetic water treatment on the calcium carbonate phase formation and the electrochemical corrosion behavior of carbon steel, J. Alloys Compd., 369 (2004) 256–259.
[2] M.-d. Cao, Z.-f. Zhou, Q. Zhang, Y.-t. Xie, S.-y. Zhang, Characteristics of physical and chemical properties and associated environmental implications of the karst water in Zhijin Cave of Guizhou Province, Carsologica Sinica, 35 (2016) 314–321+348.
[3] X.-Z. Chen, S. Li, W. Sheng, X.-L. Ren, Research progress on magnetic field scale inhibition & anti-fouling and its mechanisms, J. Eng. Therm. Energy Power, 33 (2018) 1–7.
[4] Y. Chen, Y. Cui, A.G. Barrett, F. Chille, S. Lassalle, Investigation of calcite precipitation in the drainage system of railway tunnels, Tunnelling Underground Space Technol., 84 (2019) 45–55.
[5] H. Dai, W. Xu, K. Yu, W. Wei, Concise synthesis of $NaTi_2(PO_4)_3$ nanocrystals with size and morphology control, Chin. Chem. Lett., 30 (2019) 517–520.
[6] J.D. Donaldson, S. Grimes, Lifting the scales from our pipes, New Sci., 117 (1988) 43–46.
[7] H. Duan, F. Chen, C. Yao, B. Wang, W. Shu, The phenomenon of crystal pipe blocking in karst tunnel and its induced risk, China Civ. Eng. J., 53 (2020) 332–335.
[8] C. Fan, Q. Qin, F. Liang, Z. Fan, Z. Li, Fractures in volcanic reservoirs: a case study in Zhongguai Area at the Northwestern Margin of Junggar Basin (China), Earth Sci. Res. J., 22 (2018) 169–174.
[9] D. Jiang, Z. Sintayehu, R. Fu, Experimental parameters study on prevention from descaling, J. Tianjin Univ. Sci. Technol., 23 (2008) 64–67+76.
[10] Y. Jiang, K. Du, L. Tao, J. Zhao, H. Xiao, Investigation and discussion on blocking mechanism of drainage system in karst tunnels, Railway Standard Design, 63 (2019) 131–135.
[11] J. Leal, L. Ochoa, C. Contreras, Automatic identification of calcareous lithologies using support vector machines, borehole logs and fractal dimension of borehole electrical imaging, Earth Sci. Res. J., 22 (2018) 75–82.
[12] L.C. Lipus, B. Ačko, B. Neral, Influence of magnetic water treatment on fabrics' characteristics, J. Cleaner Prod., 52 (2013) 374–379.
[13] M. Liu, Z. Xue, H. Zhang, Y. Li, Dual-channel membrane capacitive deionization based on asymmetric ion adsorption for continuous water desalination, Electrochem. Commun., 125 (2021) 106974, doi: 10.1016/j.elecom.2021.106974.
[14] S. Liu, F. Gao, Y. Zhou, Q. Liu, H. Lv, B. Wang, K. Xiang, D. Xiao, Effect of fuzz length on the prevention of crystallization of tunnel flocking drainpipes, Sci. Technol. Eng., 19 (2019) 234–239.
[15] S. Liu, X. Zhang, H. Lv, Q. Liu, B. Wang, The effect of anti-crystallization of tunnel plumage drain pipe under different water filling state, Sci. Technol. Eng., 18 (2018a) 156–163.
[16] S. Liu, X. Zhang, H. Lv, Q. Liu, B. Wang, The effect of flocking PVC pipe on the prevention and crystallization of tunnel drains, Sci. Technol. Eng., 18 (2018b) 313–319.
[17] W. Liu, Experiment and mechanism of magnetic treatment for water scale prevention, Water Wastewater Eng., 34 (2008) 62–65.
[18] Y. Luo, X. Sui, X. Huang, Research progress on the prevention and control of scale, Ind. Water Treat., 32 (2012) 18–20.
[19] D. Martin, R. Thomas, L. Albrecht, R.M. Peter, S. Peter, D. Christian, P. Gerhard, K. Dietmar, S. Herwig, Koralm tunnel as a case study for sinter formation in drainage systems – precipitation mechanisms and retaliatory action, Geomech. Tunnelling, 1 (2008) 271–278.
[20] S. Sambasivam, P.S. Maram, C.V.V.M. Gopi, I.M. Obaidat, Hydrothermal synthesis, crystal and electronic structure of a new hydrated borate $CsKB_4O_5(OH)_4{\cdot}2H_2O$, Mater. Express, 10 (2020) 543–550.
[21] M. Sun, L. Yan, L. Zhang, L. Song, J. Guo, H. Zhang, New insights into the rapid formation of initial membrane fouling after *in-situ* cleaning in a membrane bioreactor, Process Biochem., 78 (2019) 108–113.
[22] C. Tian, F. Ye, G. Song, Q. Wang, M. Zhao, B. He, J. Wang, X. Han, On mechanism of crystal blockage of tunnel drainage system and preventive countermeasures, Mod. Tunnelling Technol., 57 (2020) 66–76+83.
[23] K. Xiang, J. Zhou, X. Zhang, C. Huang, L. Song, S. Liu, Experimental study on crystallization rule of tunnel drainpipe in alkaline environment, Tunnel Constr., 39 (2019) 214–219.
[24] A. Butt, S. Umer, R. Altaf, Performance of two hybrids of *Helianthus annuus* L. (sunflower) under the stress of heavy metals i.e. zinc and copper, J. Clean WAS, 4 (2020) 8–11, doi: 10.26480/jcleanwas.01.2020.08.11.
[25] K.S. Rawat, S.K. Singh, S. Szilard, Comparative evaluation of models to estimate direct runoff volume from an agricultural watershed, Geol. Ecol. Landscapes, 5 (2021) 94–108.
[26] F. Ye, C.-m. Tian, B. He, M. Zhao, J. Wang, X.-b. Han, G.-f. Song, Experimental study on scaling and clogging in drainage system of tunnels under construction, China J. Highway Transp., 34 (2021) 159–170.
[27] F. Ye, C. Tian, M. Zhao, B. He, J. Wang, X. Han, The disease of scaling and cloging in the drainage pipes of a tunnel under construction in Yunnan, China Civ. Eng. J., 53 (2020b) 336–341.
[28] F. Ye, J. Wang, C. Tian, B. He, M. Zhao, X. Han, Y. Li, Research progress and control techniques of crystal blockage disease of tunnel drainpipe, Hazard Control Tunnelling Underground Eng., 2 (2020a) 13–22.
[29] H. Zhang, W. Guan, L. Zhang, X. Guan, S. Wang, Degradation of an organic dye by bisulfite catalytically activated with iron manganese oxides: the role of superoxide radicals, ACS Omega, 5 (2020) 18007–18012.
[30] L. Zhang, J. Zheng, S. Tian, H. Zhang, X. Guan, S. Zhu, X. Zhang, Y. Bai, P. Xu, J. Zhang, Z. Li, Effects of Al^{3+} on the microstructure and bioflocculation of anoxic sludge, J. Environ. Sci. (China), 91 (2020) 212–221.

[31] M. Zhang, L. Zhang, S. Tian, X. Zhang, J. Guo, X. Guan, P. Xu, Effects of graphite particles/Fe^{3+} on the properties of anoxic activated sludge, Chemosphere, 253 (2020) 126638, doi: 10.1016/j.chemosphere.2020.126638.
[32] X. Zhang, Y. Zhou, B. Zhang, Y. Zhou, S. Liu, Investigation and analysis on crystallization of tunnel drainage pipes in Chongqing, Adv. Mater. Sci. Eng., 2018 (2018) 7042693, doi: 10.1155/2018/7042693.
[33] Y. Zhou, X. Zhang, L. Wei, S. Liu, B. Zhang, C. Zhou, Experimental study on prevention of calcium carbonate crystallizing in drainage pipe of tunnel engineering, Adv. Civ. Eng., 2018 (2018) 9430517, doi: 10.1155/2018/9430517.
[34] Y. Zhu, Y. He, J. Gong, X. Feng, H. Peng, W. Wang, H. He, H. Liu, L. Wang, Highly stable all-inorganic $CsPbBr_3$ nanocrystals film encapsulated with alumina by plasma-enhanced atomic layer deposition, Mater. Express, 8 (2018) 469–474.